Electronic supplementary information

Induce Chirality Sensing through Formation and Aggregation of the Chiral Imines Double Winged with Pyrenes or Perylenes

Jianlin Wu,[a] Wenting Liang,[b] Tong Niu,[a] Wanhua Wu,[a*] Dayang Zhou,[c] Chunying Fan,[a] Jiecheng Ji,[a] Guowei Gao,[a*] Jian Men,[a] Yonggang Yang,[d] and Cheng Yang[a*]

[a]*Key Laboratory of Green Chemistry & Technology, College of Chemistry, State Key Laboratory of Biotherapy, West China Medical Center, and Healthy Food Evaluation Research Center, Sichuan University, 29 Wangjiang Road, Chengdu, 610064, China*

[b] *Institute of Environmental Sciences, Department of Chemistry, Shanxi University, Taiyuan 030006, P. R. China*

[c] *Comprehensive Analysis Center, ISIR, Osaka University, Mihogaoka, Ibaraki 567-0047, Japan*

[d] *Key Laboratory of Organic Synthesis of Jiangsu Province, College of Chemistry, Chemical Engineering and Materials Science, Soochow University Suzhou, China*

Contents

1. Materials and methods

All the chemicals were of analytically pure grade and were used as received. Solvents were dried and distilled before using for the synthesis. ^{1}H and ^{13}C NMR spectra were recorded at room temperature on a Bruker AMX–400 (operating at 400 MHz for ^{1}H NMR and 101 MHz for ^{13}C NMR) in $CDCl_3$ with TMS as an internal standard. HRMS were measured in a Waters Q–TOF Premiers (ESI). UV/Vis spectral studies were done on a JASCO V-650 spectrophotometer. Steady-state emission spectral studies were done on a FluoroMax-4 spectrofluoremeter (Horiba Scientific), and the data obtained were analyzed with Origin (v8.1) integrated software FluoroEssence (v2.2). Circular Dichroism (CD) studies were done on a JASCO CD spectropolarimeter (model-J1500). Dynamic light scattering (DLS) studies were done on a Zetasizer Nano ZS90. Scanning electron microscope (SEM) studies were done on a Hitachi Su500 instrument.

2. Synthetic procedures for sensors 1 and 2

2.1 Synthesis of 3,5-diethynylbenzaldehyde

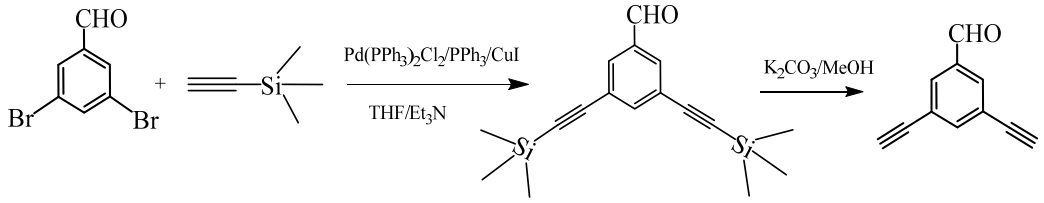

Under an argon atmosphere, 3, 5-dibromobenzaldehyde (1.96 g, 7.42 mmol), $Pd(PPh_3)_2Cl_2$ (260 mg, 0.37 mmol), CuI (70 mg, 0.37 mmol) and PPh_3 (193 mg, 0.74mmol) were dissolved in 80 mL anhydrous THF/Et_3N (1:1, v:v). The flask was vacuumed and back-filled with argon for several times and the mixture was stirred for ca. 15 min at room temperature, then trimethylsilylacetylene (2.19 g, 22.26 mmol) was added via syringe. The solution was refluxed for 7 h. Then the solvent was removed under a reduced pressure, and the residue was purified by column chromatography on silica gel (hexane as the eluent) to give 3,5-bis(trimethylsilylethynyl)benzaldehyde 2.0 g (yield: 90.9%) as a colorless oil.

The above trimethylsilane protected intermediate (2.0 g, 6.70 mmol) was dissolved in methanol (30 mL), to which K_2CO_3 (500 mg, 3.62 mmol)) was added and the mixture was stirred for 2 h at room temperature. The reaction mixture was then concentrated under vacuum, and the residue 1.6 H was purified by silica gel chromatography to give 3,5-diethynylbenzaldehyde (750 mg, 70% yield) as white solid. ^{1}H NMR (400 MHz, $CDCl_3$): δ 10.0 (s, 1H), 8.0 (d, J =1.6 Hz, 2H), 7.8 (t, J = 1.6 Hz, 1H), 3.0 (s, 2H). Literature data[1], ^{1}H NMR ($CDCl_3$): δ 9.97 (s, 1 H), 7.95 (d, 2 H, J = 1.5 Hz), 7.82 (t, 1 H, J = 1.5 Hz), 3.19 (s, 2 H).

2.2 Synthesis of compound **1**

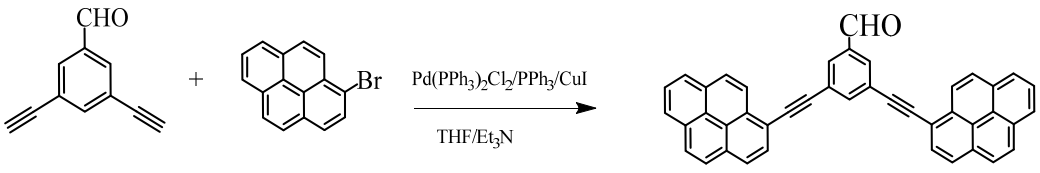

1

Under an argon atmosphere, 3,5-diethynylbenzaldehyde (200 mg, 1.30 mmol) and 1-bromopyrene (911 mg, 3.24 mmol) were dissolved in 60 mL anhydrous THF/Et_3N (2:1, v:v). Then. a mixture of $Pd(PPh_3)_2Cl_2$(45.62 mg, 0.065 mmol), PPh_3 (34.08 mg, 0.13mmol) and CuI (24.74 mg, 0.13 mmol, 10 mol %) were added. The mixture was refluxed for 24 h, and then the solvent was evaporated under a reduced pressure. The crude product was purified by column chromatography (silica gel, hexanes/CH_2Cl_2 (1:1) eluent) to give compound **1** (60 mg, 8.35% yield) as light yellow solid. ^{1}H NMR ($CDCl_3$, 400 MHz), δ 10.12 (s, 1H), 8.70 (d, *J* = 9.1 Hz, 2H), 8.28-8.25 (m, 9H), 8.20 – 8.11 (m, 6H), 8.08 (dd, *J* = 8.3, 4.4 Hz, 4 H). ^{13}C NMR ($CDCl_3$, 100 MHz) δ 191.3, 139.7, 137.1, 132.6, 132.5, 132.4, 132.2, 132.0, 131.5, 131.3, 130.1, 128.9, 128.8, 128.8, 128.7, 127.4, 126.6, 126.2, 126.1, 125.6, 125.5, 124.8, 124.7, 124.5, 117.0, 93.1, 91.2. HRMS (ESI): calcd ($[C_{43}H_{22}O]^+$), $[M+Na]^+$: 557.1671; found: $[M+Na]^+$: 557.1800.

2.2 Synthesis of compound **2**

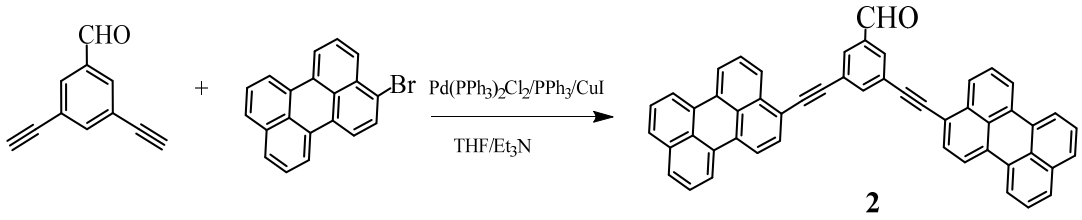

2

Under an argon atmosphere, 3,5-diethynylbenzaldehyde (60.0 mg, 0.38 mmol) and 1-bromoperylene (308.5 mg, 0.93mmol) were dissolved in anhydrous THF/Et_3N (2:1, 80 mL) solution. Then, a catalyst mixture of $Pd(PPh_3)_2Cl_2$ (45.6 mg, 0.065 mmol, 5 mol %), PPh_3 (34.1 mg, 0.13mmol 10 mol %), and CuI (24.7 mg, 0.13 mmol, 10 mol %) was added under argon. The mixture was refluxed for 24 h at 90 ºC. The solvent was evaporated under a reduced pressure. The crude product was purified by column chromatography (silica gel, hexanes/ CH_2Cl_2 = 1/1 as the eluent) to give 15 mg light yellow solid (Yield: 5.89%). ^{1}H NMR ($CDCl_3$,400 MHz) δ 10.02 (s, 1H), 8.36 – 7.86 (m, 12H), 7.84 – 7.38 (m, 10H), 7.35 (d, *J* = 2.3 Hz, 1H), 7.13 (dd, *J* = 8.6, 2.5 Hz, 2H). ^{13}C NMR ($CDCl_3$, 100 MHz) δ 190.8, 140.1, 136.8, 134.7, 132.6, 132.5, 131.6, 128.8, 128.4, 127.7, 126.9, 126.8, 126.0, 125.2, 124.6, 124.1, 123.9, 121.3, 121.0, 120.9, 119.7, 119.3, 81.6, 79.6. ESI-HRMS: calcd ($[C_{51}H_{26}O]^+$): 654.1984; found: 654.0506.

3. Structure characterization data

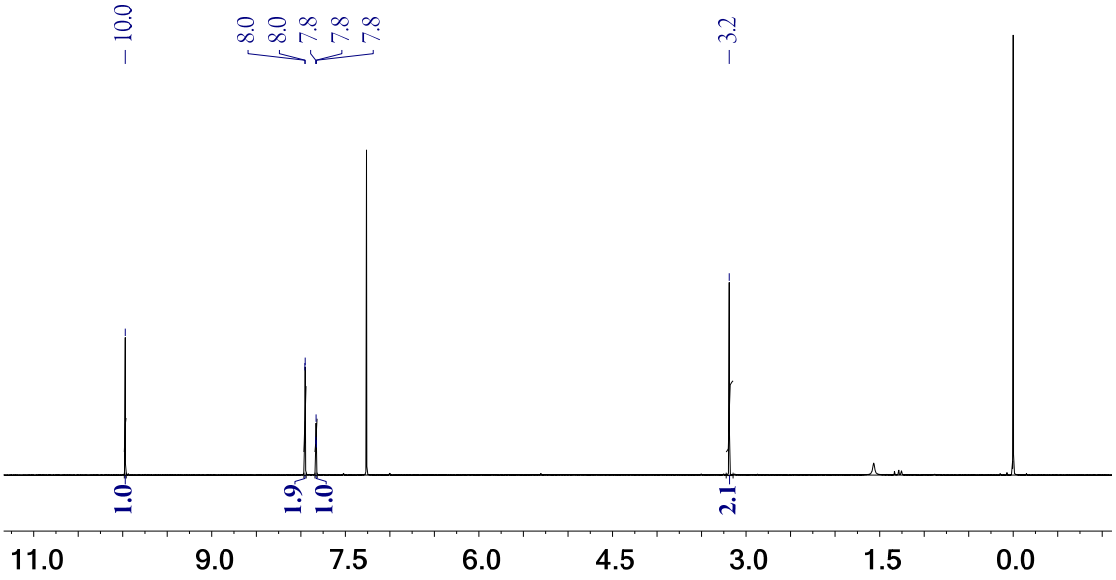

Fig. S1 ^{1}H NMR spectrum (400 MHz, $CDCl_3$, room temperature) of 3,5-diethynylbenzaldehyde.

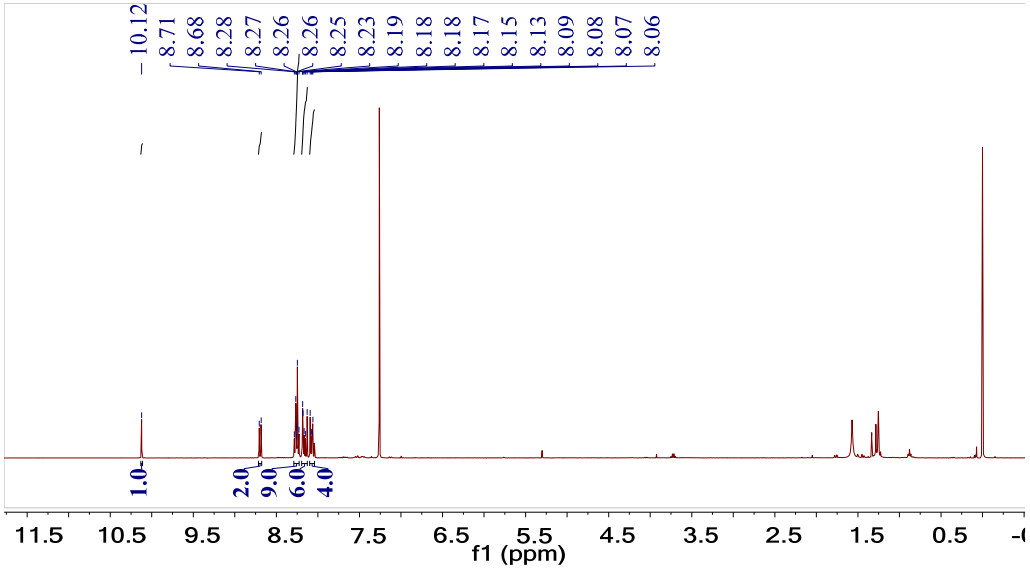

Fig. S2 ^{1}H NMR spectrum (400 MHz, $CDCl_3$, room temperature) of compound **1**.

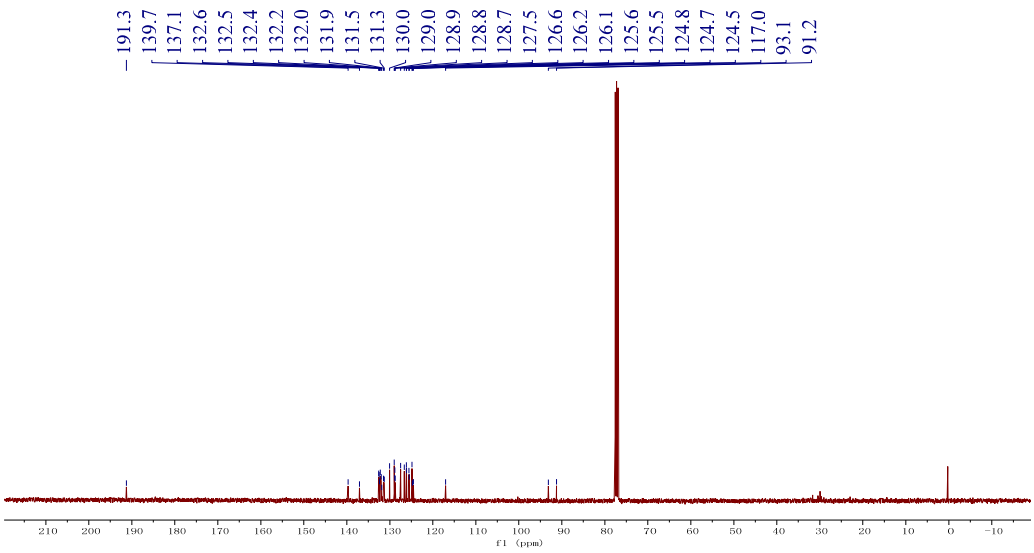

Fig. S3 ^{13}C NMR spectrum (100 MHz, $CDCl_3$, room temperature) of compound **1**.

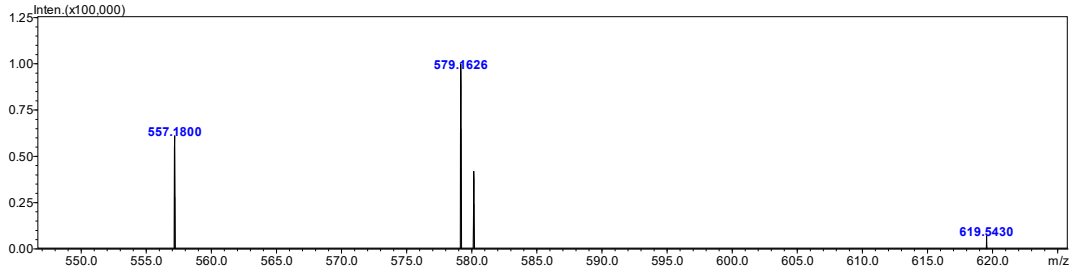

Fig. S4 HRMS of compound **1.**

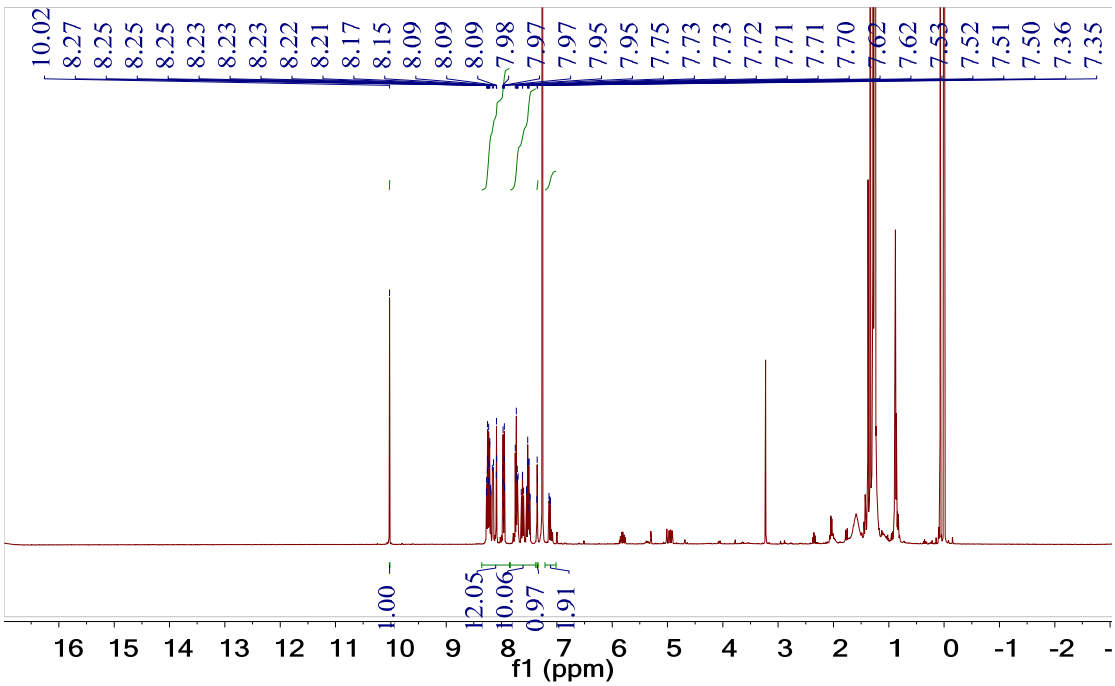

Fig. S5 ^{1}H NMR spectrum (400 MHz, $CDCl_3$, room temperature) of compound **2**.

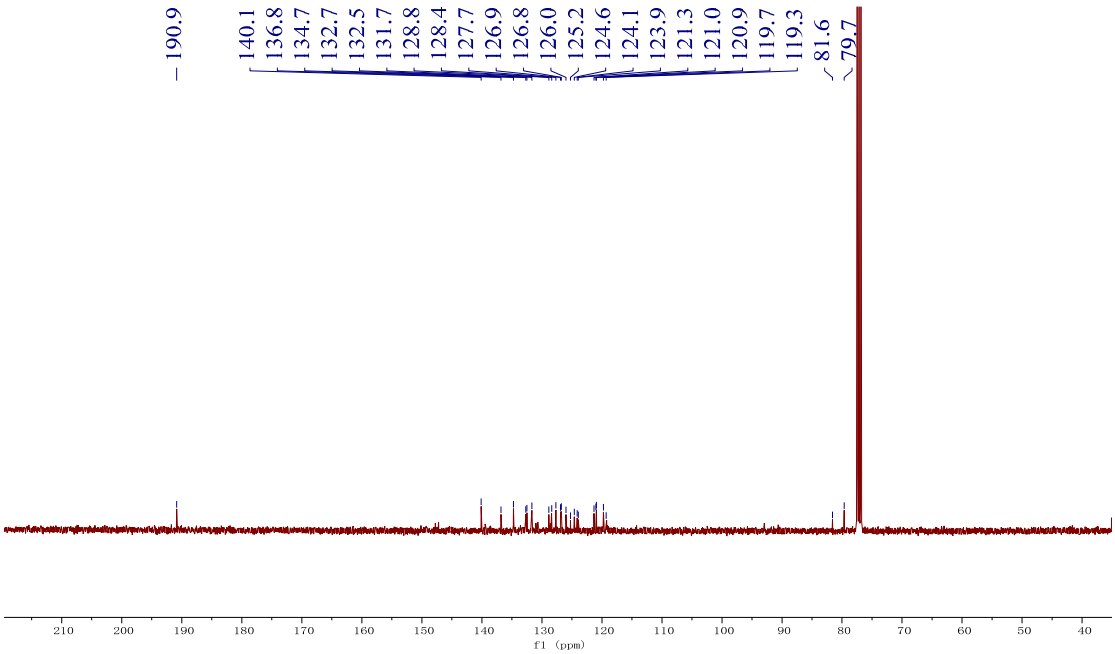

Fig. S6 ^{13}C NMR spectrum (100 MHz, $CDCl_3$, room temperature) of compound **2**.

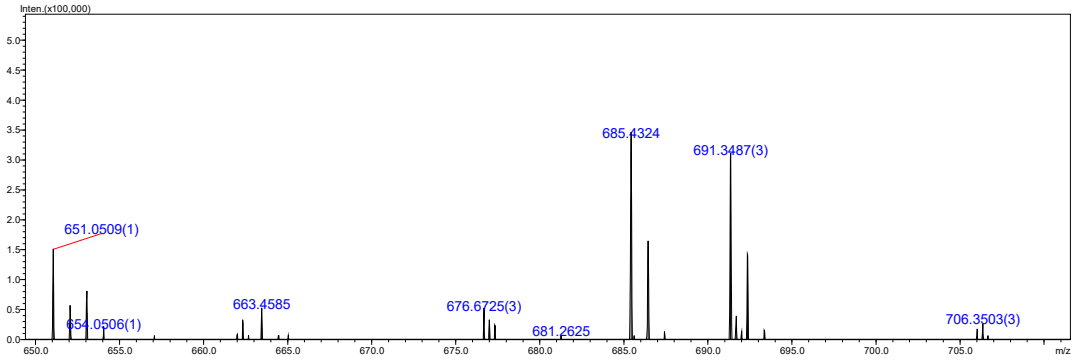

Fig. S7 HRMS of compound **2**.

4. Photophysical properties of sensors 1 and 2

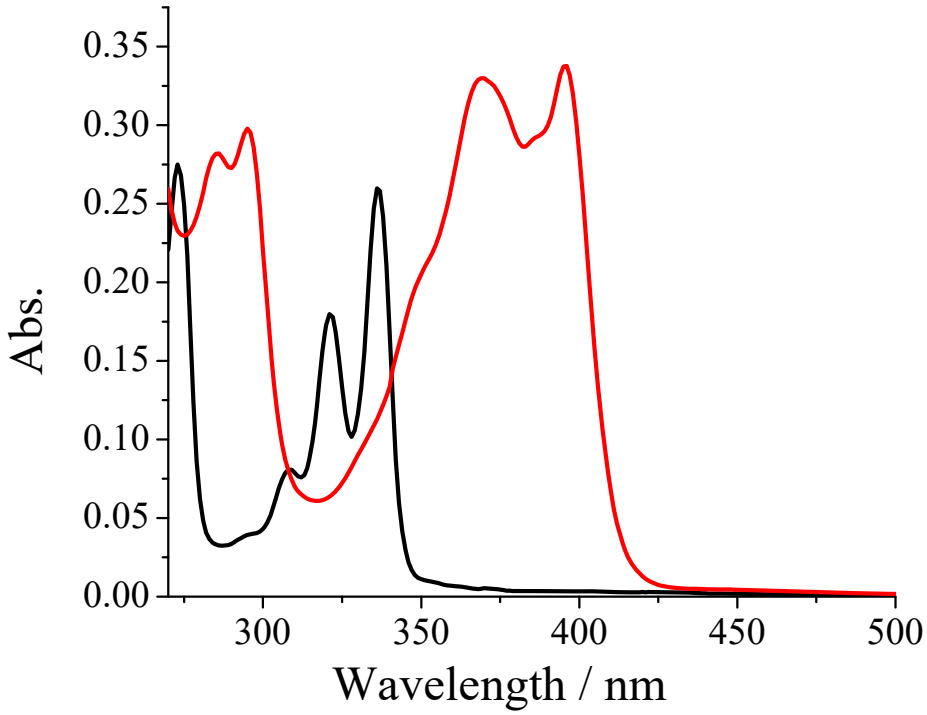

Fig. S8. UV−vis spectra of pyrene (black) and sensor **1** (red) (1×10^{-5} M) in DMF at 25 °C.

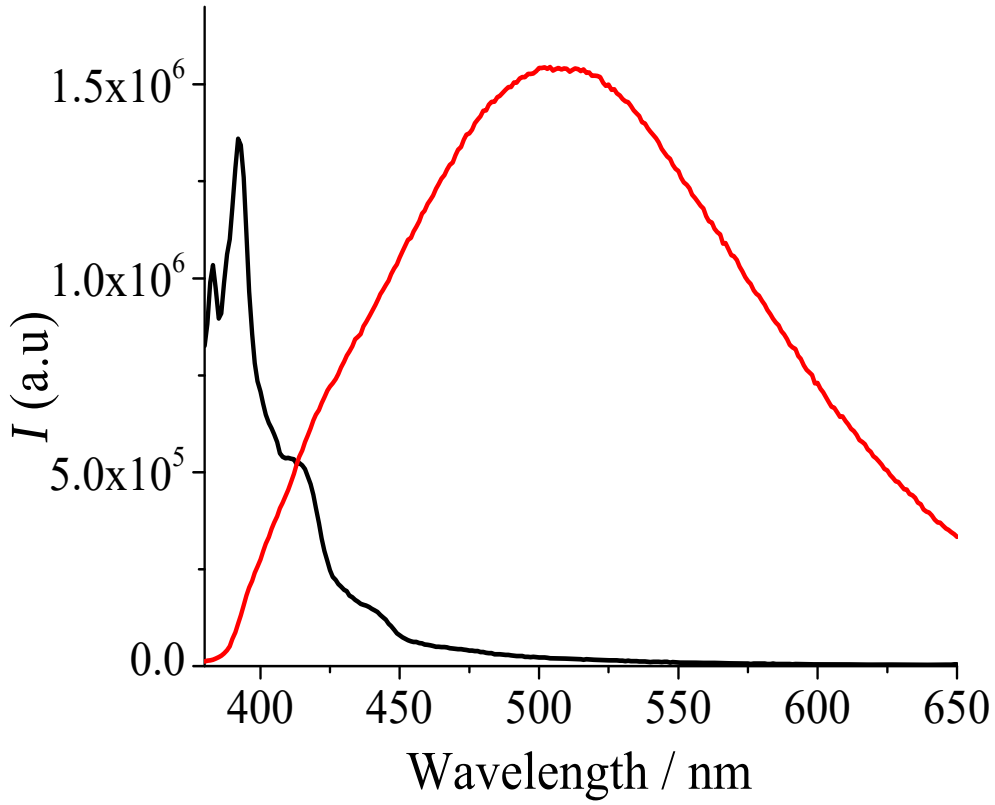

Fig. S9. Fluorescence spectra of pyrene (black) and sensor **1** (red) (3.0×10^{-6} M) in DMF at 25 °C; λ_{ex} = 370 nm.

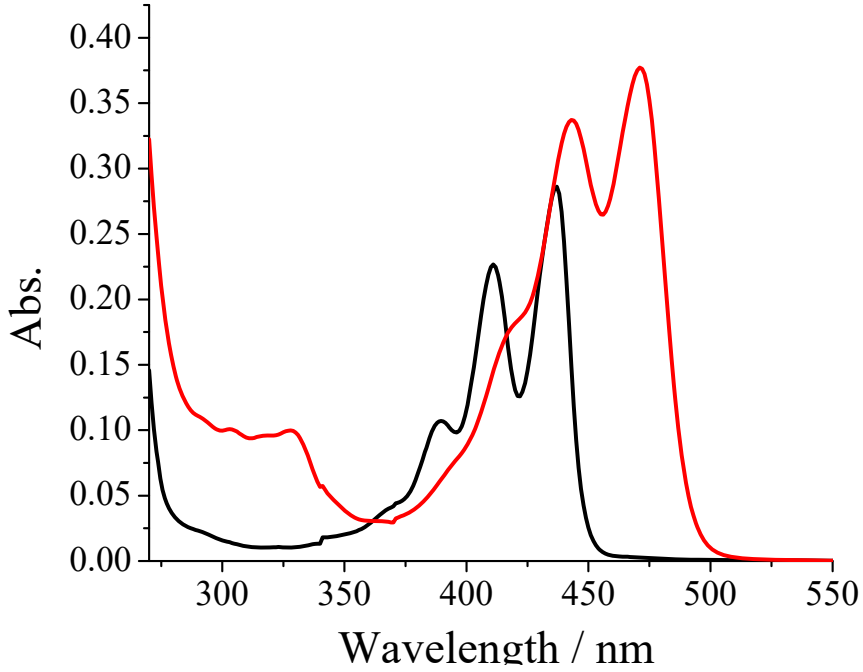

Fig. S10. UV−vis absorption spectra of perylene (black) and sensor **2** (red) (1×10^{-5} M) in DMF at 25 °C.

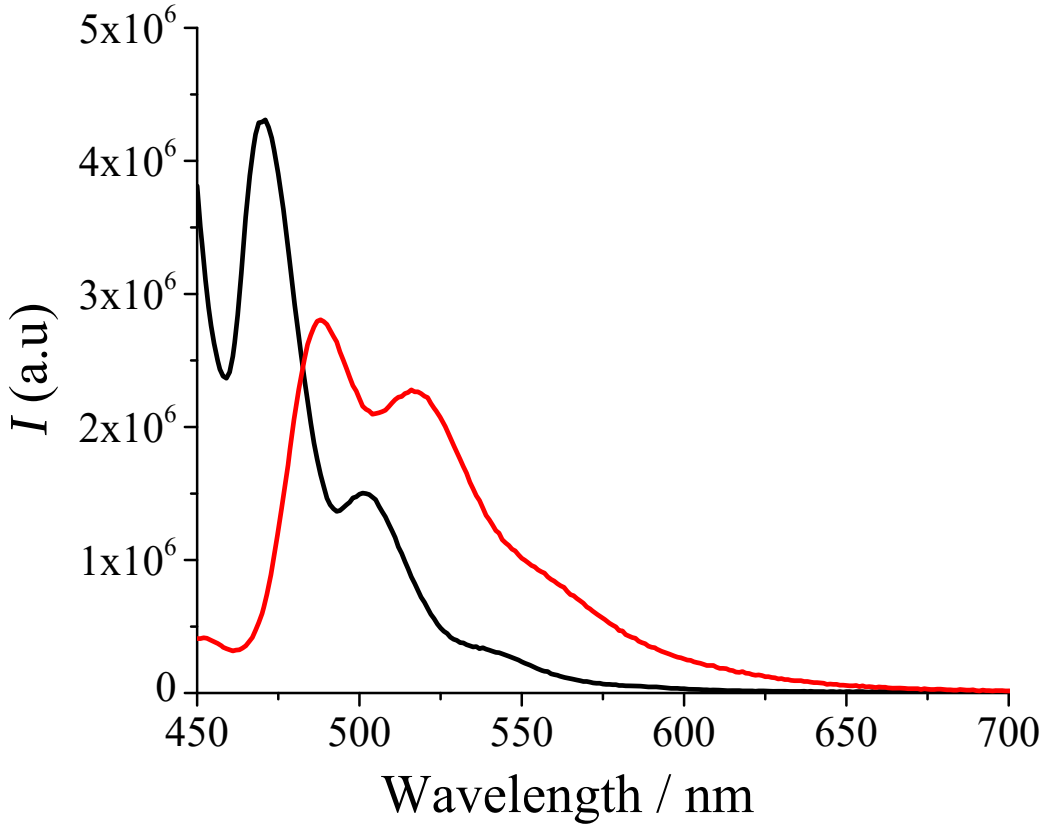

Fig. S11. Fluorescence spectra of perylene (black) and sensor **2** (red) (3.0×10^{-6} M) in DMF at 25 °C; $\lambda_{ex} = 440$ nm.

5. Characterization of the formation of imine from 1 and (*R*)-A2

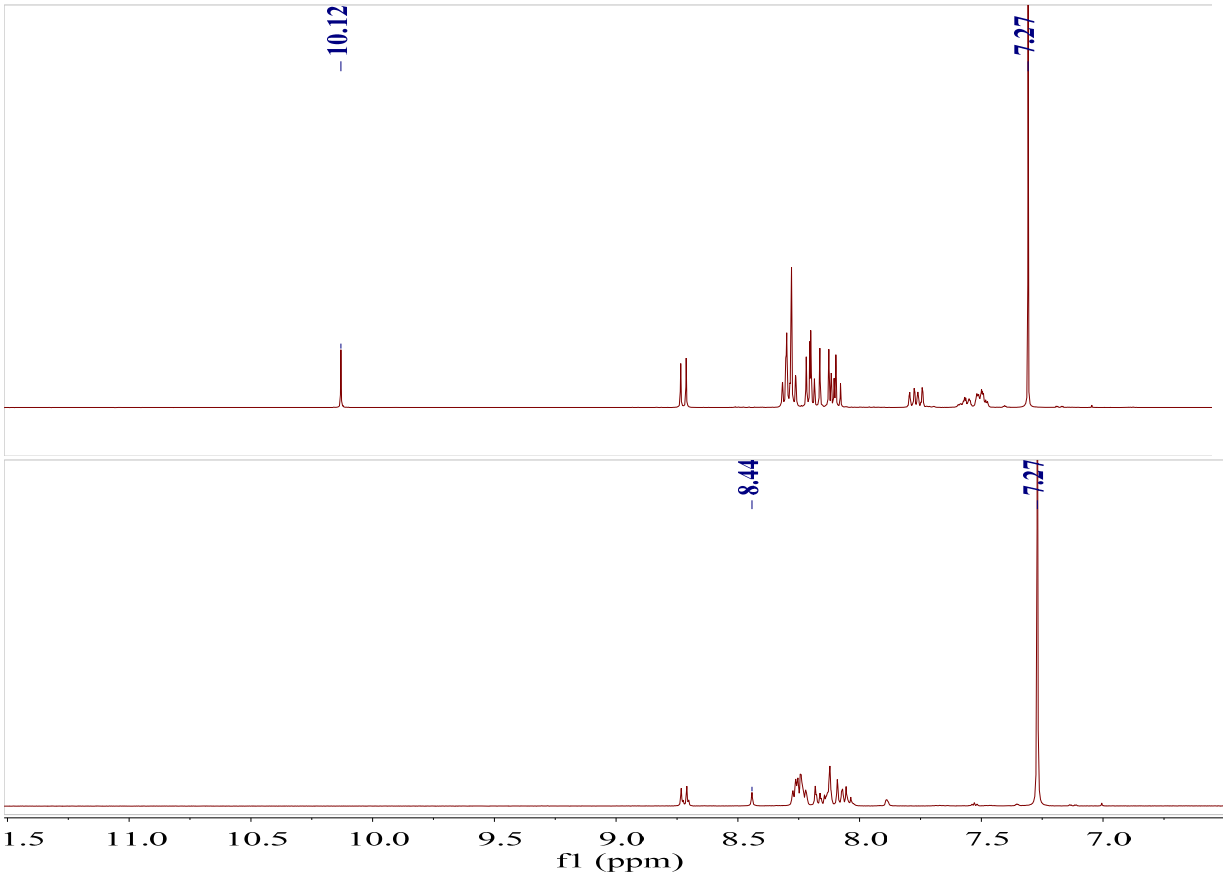

Fig. S12. Partial ^{1}H NMR spectra (400 MHz, $CDCl_3$) for the formation of imine from **1** and (*R*)-**A2**.

6. The characterization of aggregates of imine formed by 2 with A6

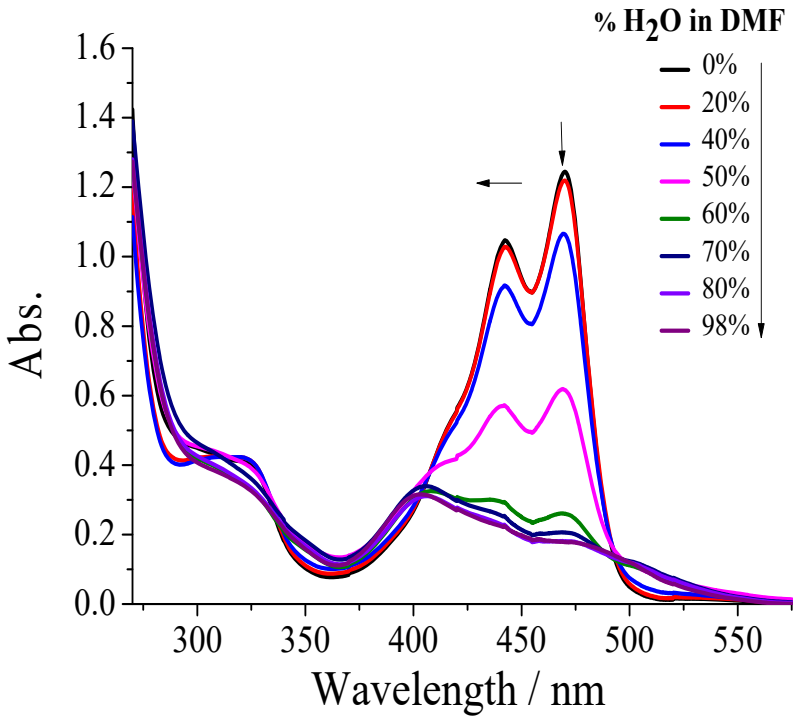

Fig. S13. Water content-dependent UV−vis spectra of the chiral imine (40 μM) derived from the reaction of **2** with **A6** in DMF for 30 min.

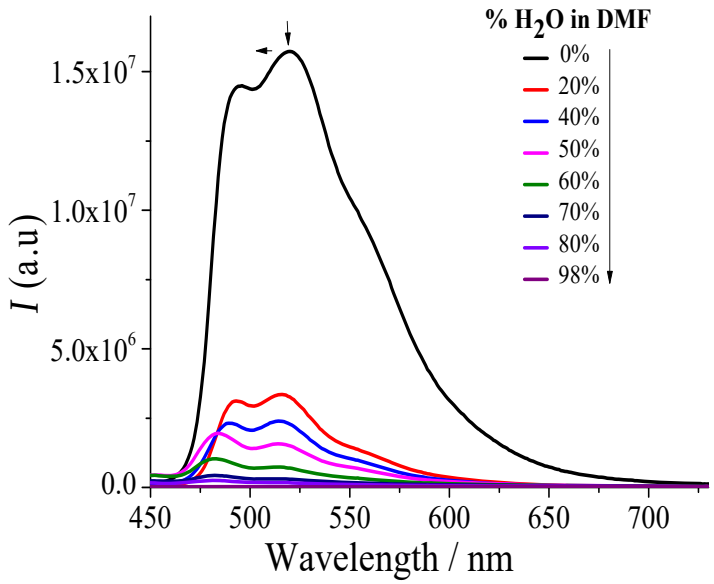

Fig. S14. Water content-dependent fluorescence of the chiral imine (40 μM) derived from the reaction of **2** with **A6** in DMF for 30 min.

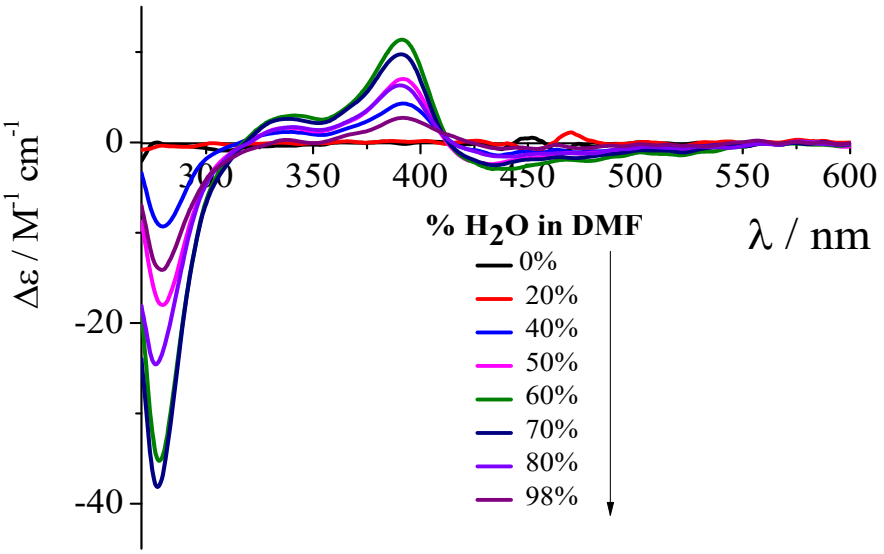

Fig. S15. Water content-dependent CD spectra of the chiral imine (40 μM) derived from the reaction of **2** with **(S)-A6** in DMF for 30 min.

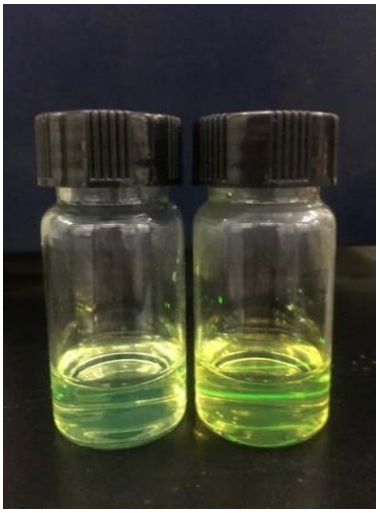

Fig. S16. Light scattering of the chiral imine (40 μM) derived from **2** and **A6** in DMF (left) and in 1:1 (v/v) DMF/H_2O (right).

Fig. S17 Emission of the chiral imine (40 μM) derived from **2** and **A6** in DMF (left) and 1:1 (v/v) DMF/H_2O (right).

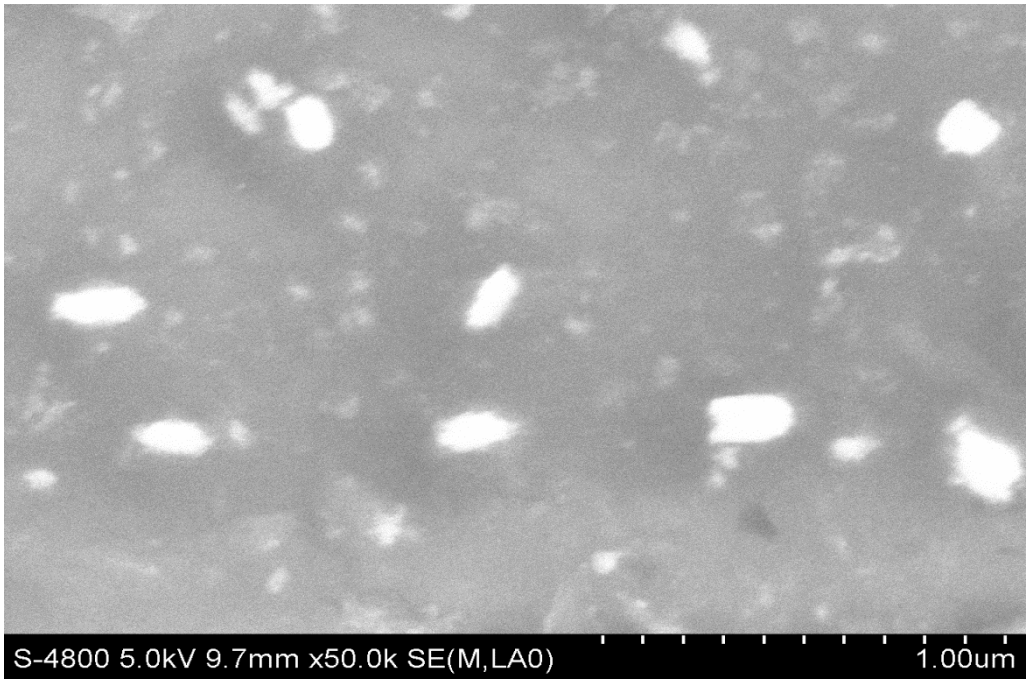

Fig. S18. SEM image of the imine derived from **2** and **A6** aggregated in 1:1 (v/v) DMF/H_2O.

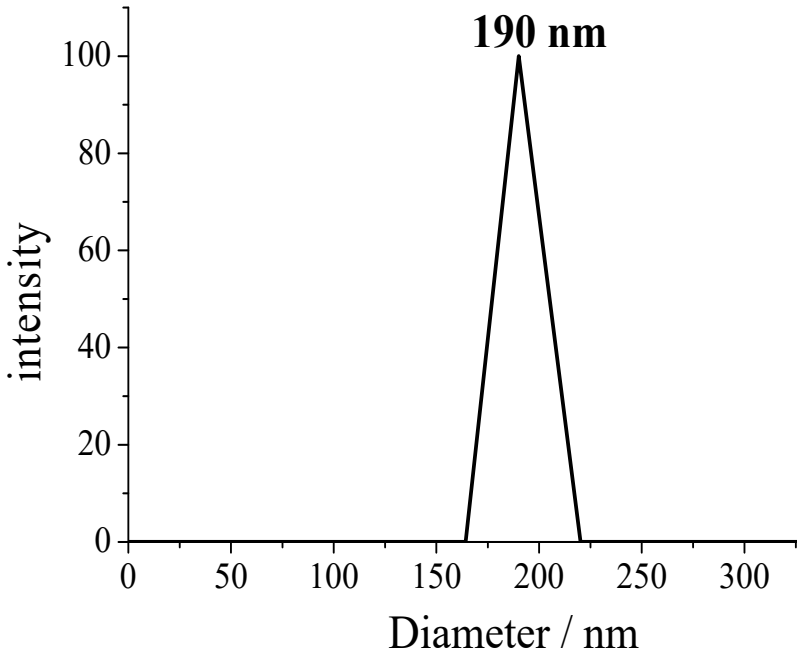

Fig. S19. DLS measurements of the imine derived from **2** and **A6** aggregated in 1:1 (v/v) DMF/H_2O.

7. Chiroptical sensing with sensors 1 and 2

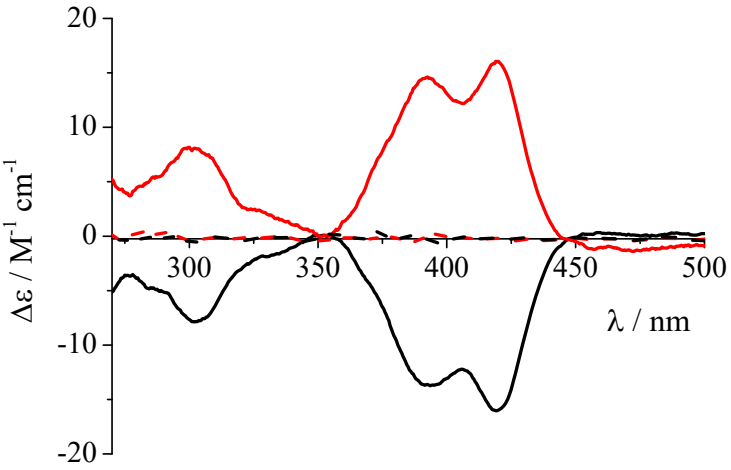

Fig. S20. CD spectra of 50 μM chiral imines derived from **1** and **A2** at 25 °C. Red and black lines represent the CD spectra of chiral imines derived from (*R*)- and (*S*)-amines, respectively, while broken and solid lines represent the CD spectra measured in DMF and in 1:1 (v/v) DMF/H_2O, respectively.

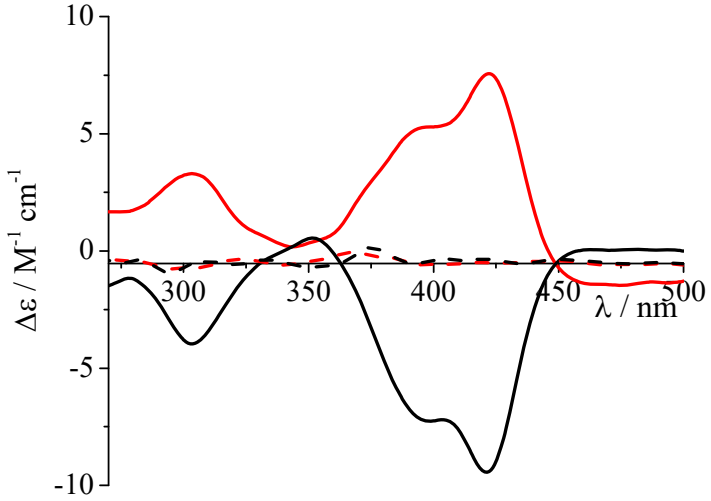

Fig. S21. CD spectra of 50 μM chiral imines derived from **1** and **A3** at 25 °C. Red and black lines represent the CD spectra of chiral imines derived from (*R*)- and (*S*)-amines, respectively, while broken and solid lines represent the CD spectra measured in DMF and in 1:1 (v/v) DMF/H_2O, respectively.

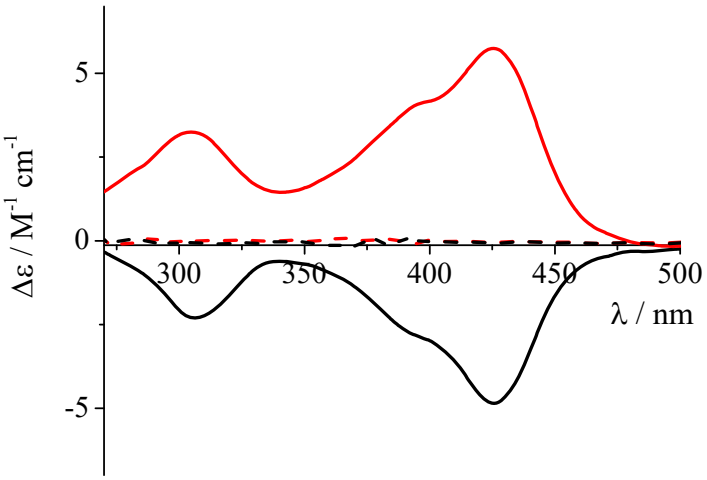

Fig. S22. CD spectra of 50 μM chiral imines derived from **1** and **A4** at 25 °C. Red and black lines represent the CD spectra of chiral imines derived from (*R*)- and (*S*)-amines, respectively, while broken and solid lines represent the CD spectra measured in DMF and in 1:1 (v/v) DMF/H_2O, respectively.

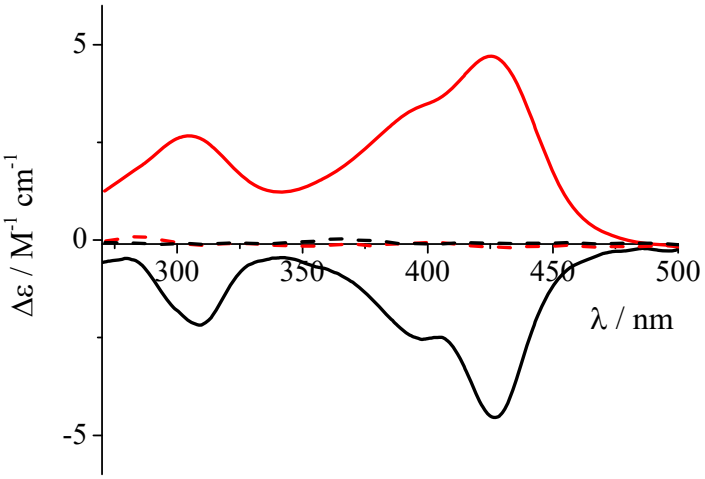

Fig. S23. CD spectra of 50 μM chiral imines derived from **1** and **A6** at 25 °C. Red and black lines represent the CD spectra of chiral imines derived from (*R*)- and (*S*)-amines, respectively, while broken and solid lines represent the CD spectra measured in DMF and in 1:1 (v/v) DMF/H_2O, respectively.

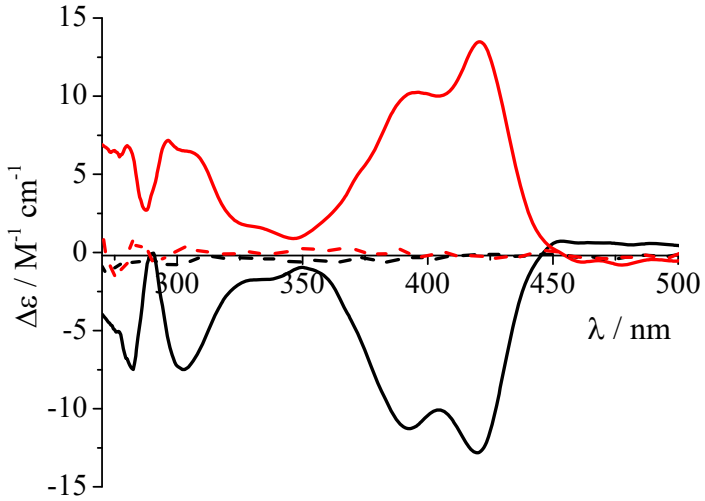

Fig. S24. CD spectra of 50 μM chiral imines derived from **1** and **A7** at 25 °C. Red and black lines represent the CD spectra of chiral imines derived from (*R*)- and (*S*)-amines, respectively, while broken and solid lines represent the CD spectra measured in DMF and in 1:1 (v/v) DMF/H_2O, respectively.

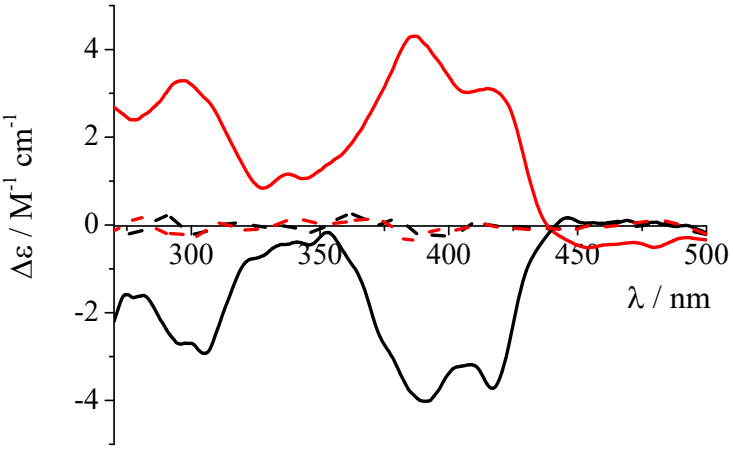

Fig. S25 CD spectra of 50 μM chiral imines derived from **1** and **A8** at 25 °C. Red and black lines represent the CD spectra of chiral imines derived from (*R*)- and (*S*)-amines, respectively, while broken and solid lines represent the CD spectra measured in DMF and in 1:1 (v/v) DMF/H_2O, respectively.

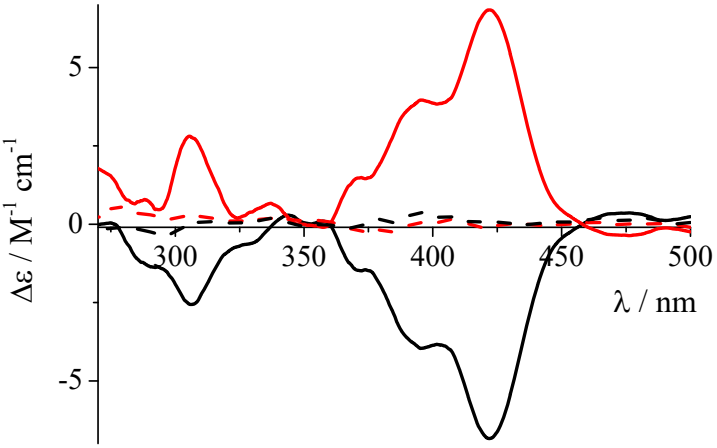

Fig. S26 CD spectra of 50 μM chiral imines derived from **1** and **A9** at 25 °C. Red and black lines represent the CD spectra of chiral imines derived from (*R*)- and (*S*)-amines, respectively, while broken and solid lines represent the CD spectra measured in DMF and in 1:1 (v/v) DMF/H_2O, respectively.

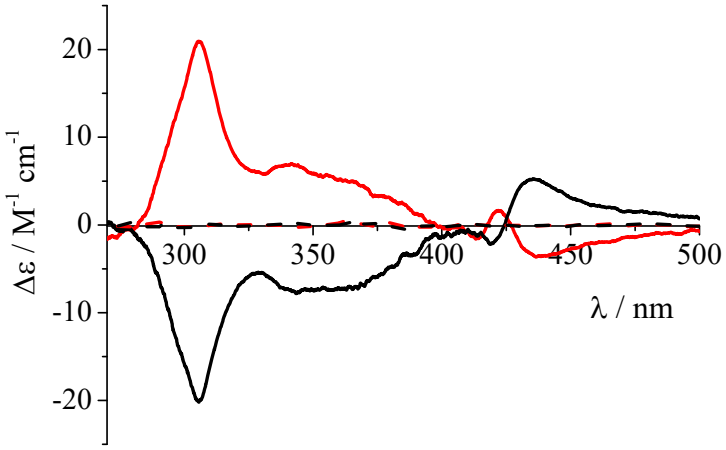

Fig. S27 CD spectra of 50 μM chiral imines derived from **1** and **A10** at 25 °C. Red and black lines represent the CD spectra of chiral imines derived from (*R*)- and (*S*)-amines, respectively, while broken and solid lines represent the CD spectra measured in DMF and in 1:1 (v/v) DMF/H_2O, respectively.

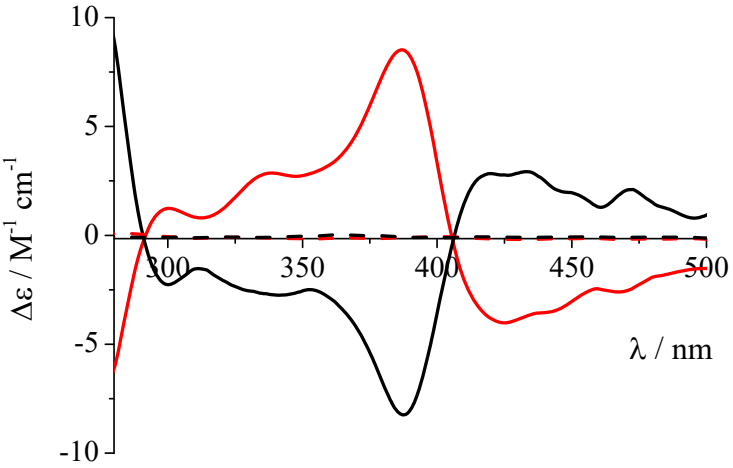

Fig. S28. CD spectra of 50 μM chiral imines derived from **2** and **A1** at 25 °C. Red and black lines represent the CD spectra of chiral imines derived from (*R*)- and (*S*)-amines, respectively, while broken and solid lines represent the CD spectra measured in DMF and in 1:1 (v/v) DMF/H_2O, respectively.

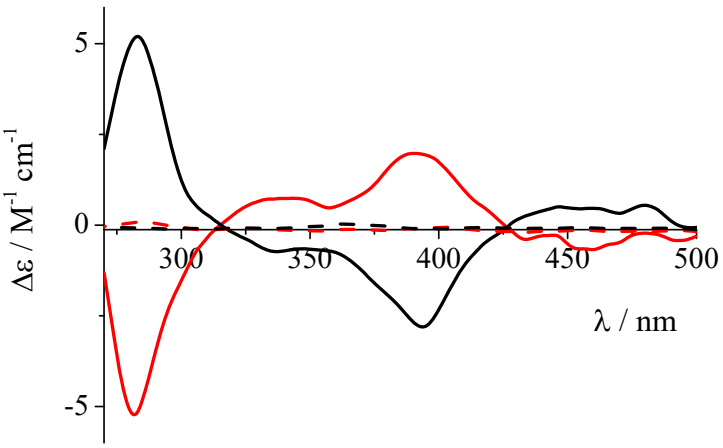

Fig. S29. CD spectra of 50 μM chiral imines derived from **2** and **A2** at 25 °C. Red and black lines represent the CD spectra of chiral imines derived from (*R*)- and (*S*)-amines, respectively, while broken and solid lines represent the CD spectra measured in DMF and in 1:1 (v/v) DMF/H_2O, respectively.

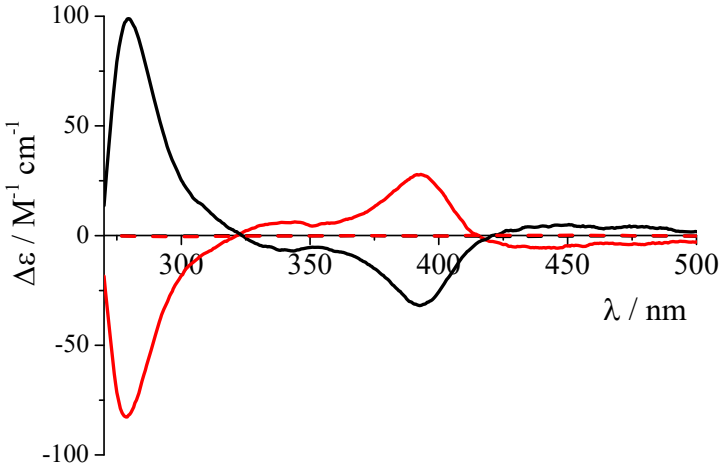

Fig. S30. CD spectra of 50 μM chiral imines derived from **2** and **A3** at 25 °C. Red and black lines represent the CD spectra of chiral imines derived from (*R*)- and (*S*)-amines, respectively, while broken and solid lines represent the CD spectra measured in DMF and in 1:1 (v/v) DMF/H_2O, respectively.

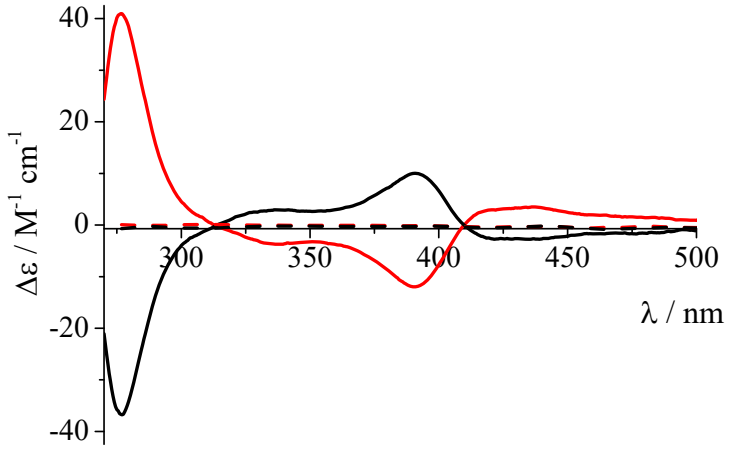

Fig. S31. CD spectra of 50 μM chiral imines derived from **2** and **A4** at 25 °C. Red and black lines represent the CD spectra of chiral imines derived from (*R*)- and (*S*)-amines, respectively, while broken and solid lines represent the CD spectra measured in DMF and in 1:1 (v/v) DMF/H_2O, respectively.

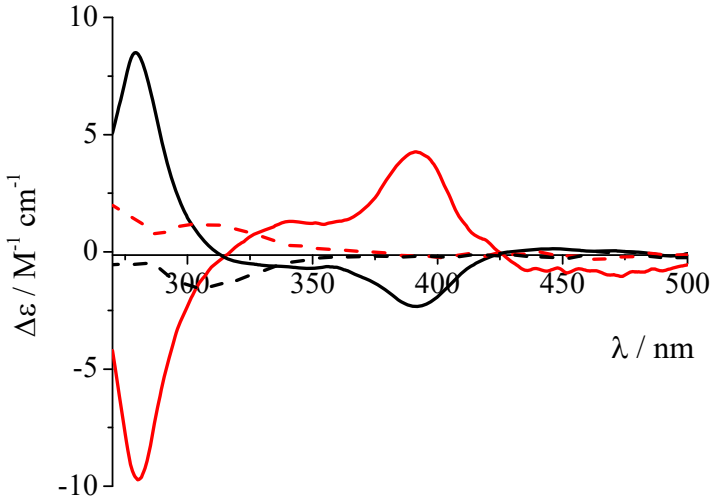

Fig. S32. CD spectra of 50 μM chiral imines derived from **2** and **A5** at 25 °C. Red and black lines represent the CD spectra of chiral imines derived from (*R*)- and (*S*)-amines, respectively, while broken and solid lines represent the CD spectra measured in DMF and in 1:1 (v/v) DMF/H_2O, respectively.

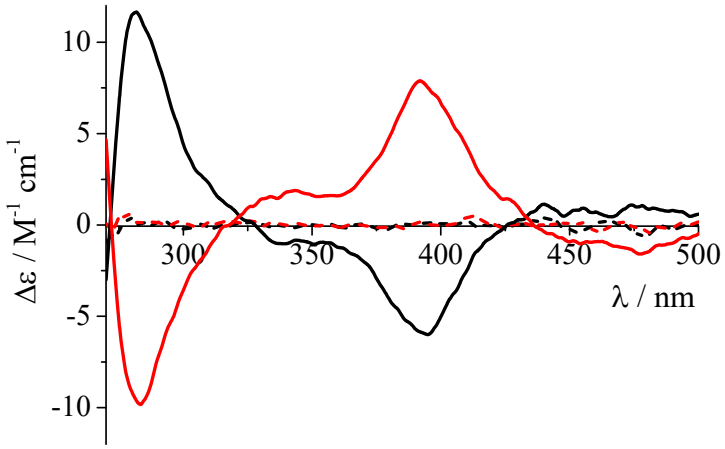

Fig. S33 CD spectra of 50 μM chiral imines derived from **2** and **A9** at 25 °C. Red and black lines represent the CD spectra of chiral imines derived from (*R*)- and (*S*)-amines, respectively, while broken and solid lines represent the CD spectra measured in DMF and in 1:1 (v/v) DMF/H_2O, respectively.

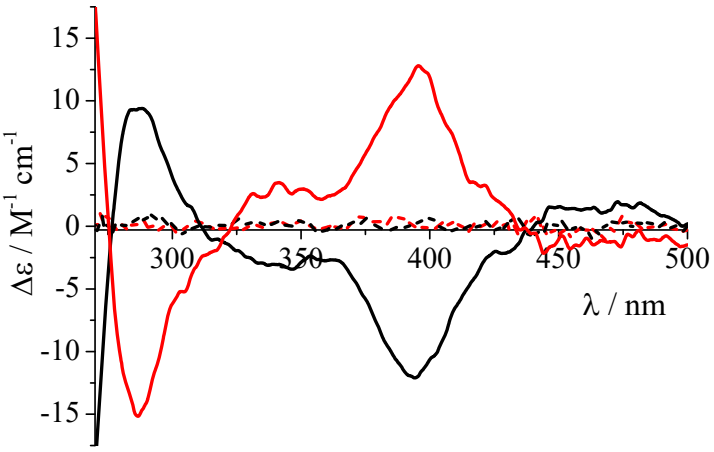

Fig. S34 CD spectra of 50 μM chiral imines derived from **2** and **A10** at 25 °C. Red and black lines represent the CD spectra of chiral imines derived from (*R*)- and (*S*)-amines, respectively, while broken and solid lines represent the CD spectra measured in DMF and in 1:1 (v/v) DMF/H_2O, respectively.

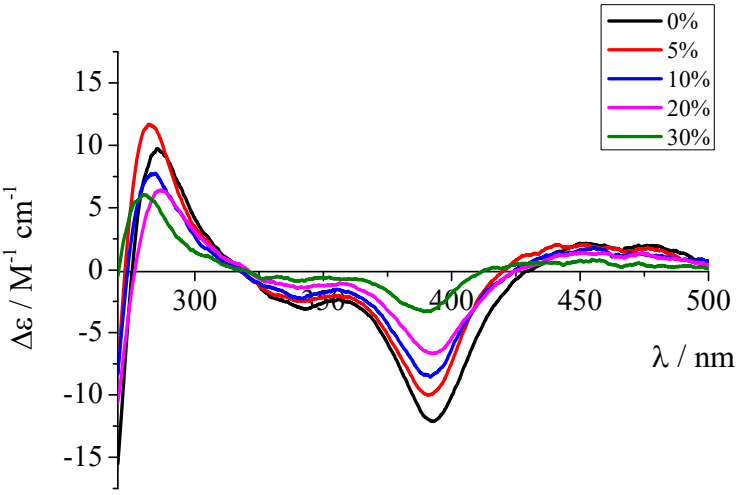

Fig. S35 CD spectra of 50 μM chiral imines obtained by reacting **2** with (*S*)-**A10** in the presence of 0-30% achiral *n*-butylamine in DMF; measured in 1:1 (v/v) DMF/H_2O at 25 °C.

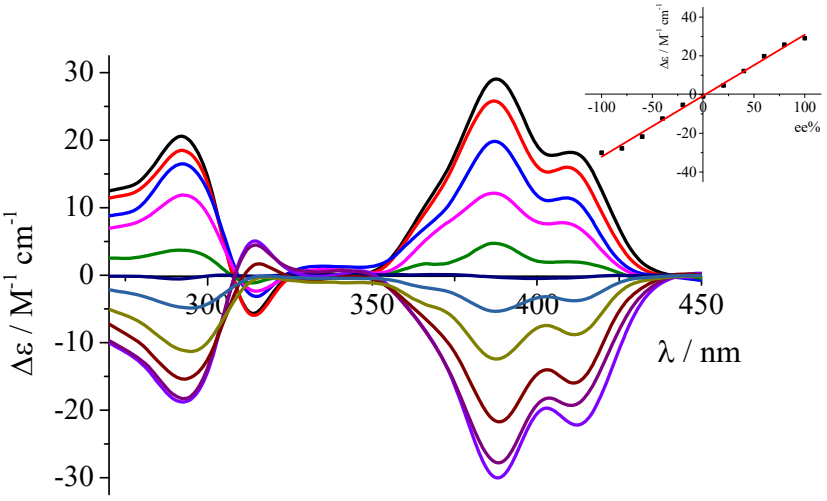

Fig. S36 CD spectra of the imines (40 μM) obtained by reacting **1** with **A1** of different *ee*'s in DMF; measured in 1:1 (v/v) DMF/H_2O at 25 °C. Inset: Plot of the ellipticity at 390 nm as a function of *ee*.

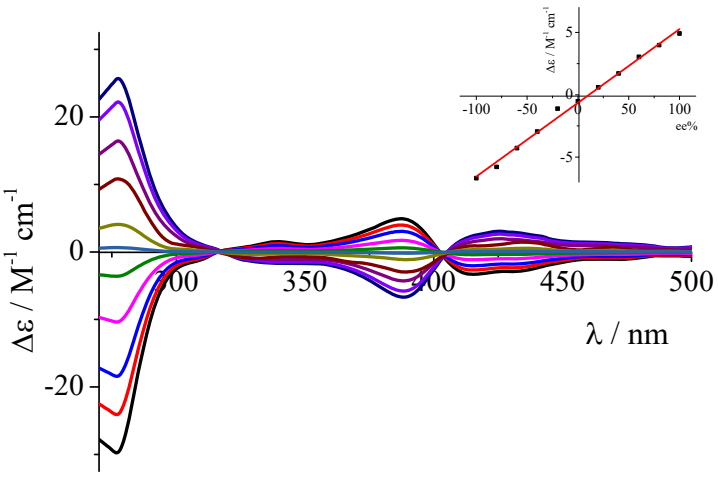

Fig. S37 CD spectra of the imine (40 μM) obtained by reacting **2** with **A4** of different *ee*'s in DMF; measured in 1:1 (v/v) DMF/H_2O at 25 °C. Inset: Plot of the ellipticity at 390 nm as a function of *ee*.

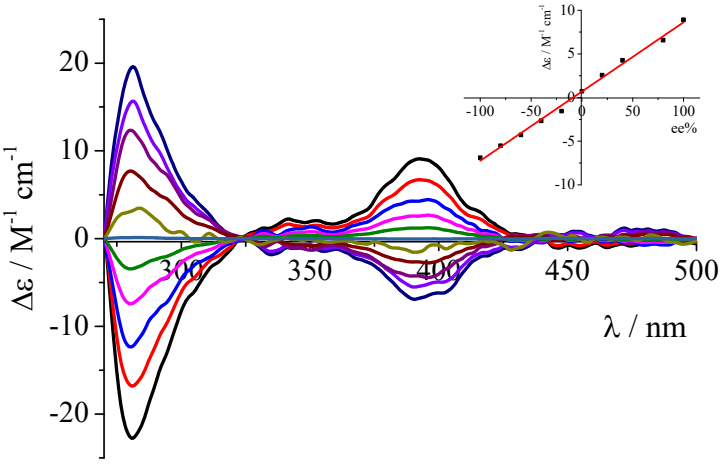

Fig. S38 CD spectra of the imine (20 μM) obtained by reacting **2** with **A3** of different *ee*'s in DMF; measured in 1:1 (v/v) DMF/H_2O at 25 °C. Insert: Plot of the ellipticity at 390 nm as a function of *ee*.

Table S1. The *ee* determination of amines **A1** and **A5** with sensor **1** and of **A3** and **A4** with **2** using the calibration line for each analyte (Figs. 3 and S37-S39)

Sensor	Chiral amine	% ee	$\Delta\varepsilon$ /M^{-1} cm^{-1}	% *ee* calculated	Error in % *ee*	Average error
1	**A1**	88.0	25.7	85.9	2.1	2.1
		66.7	20.2	66.1	0.6	
		48.0	13.8	46.8	1.2	
		-28.0	-11.2	-32.3	4.3	
		-12.0	-2.5	-9.7	2.3	
	A5	86.7	14.7	84.2	2.5	2.7
		66.7	10.9	63.6	3.1	
		-76.0	-14.6	-73.4	2.6	
		-46.0	-9.0	-45.7	0.3	
		-12.0	-4.1	-16.8	4.8	
2	**A3**	76.0	6.2	71.0	5.0	2.4
		26.0	2.8	27.7	1.7	
		-88.0	-6.2	-86.4	1.6	
		-66.7	-4.7	-67.1	0.4	
		-16.0	-0.9	-19.5	3.5	
	A4	78.0	3.9	76.2	1.8	2.4
		66.7	3.3	66.5	0.2	
		44.0	2.1	47.7	3.7	
		86.7	-5.6	-83.9	2.8	
		24.0	-2.2	-27.3	3.3	

8. Reference

[1] E. Díez-Barra, J. C. García-Martínez, J. Rodríguez-López, *J. Org. Chem.*, **2003**, *68*, 832–838